

1 *Replies to Interactive comment on “Influence of regional precipitation*
2 *patterns on stable isotopes in ice cores from the central Himalayas” by*
3 **H. Pang et al.**

4
5 **Note: The reviewer’s comments are in black, and our replies in blue.**

6
7 Anonymous Referee #3

8
9 With this study the authors addressed the question why the stable isotope records of two ice cores
10 from nearby sites in the Central Himalayas are interpreted differently. Whereas the record from
11 East Rongbuk (ER) Glaciers is interpreted as precipitation sensitive, the record from Dasuopu
12 (DSP) Glacier is thought to reflect temperature. The different behavior is explained by distinct
13 precipitation patterns with a higher contribution of the Indian Summer Monsoon to the ER Glacier,
14 resulting in an amount effect. In contrast, the Dasuopu Glacier also receives precipitation
15 associated with winter westerlies. These results were obtained from EOF and correlation analysis
16 of the ice core data sets with regional instrumental summer monsoon rainfall data in India.

17 This is an important topic and answering this question would have strong implications for future
18 interpretations of ice core stable isotope records as stated in the abstract. However, the study does
19 not totally meet the expectations and does not succeed in resolving the contradiction. There is no
20 clear evidence for a relation between ice core data and instrumental data as outlined below. The
21 findings are in contrast to previous publications, which is not discussed. The information given for
22 the ice core data is not sufficient and the data is not critically evaluated, see below. I therefore
23 think the paper needs major revisions.

24 Neither the EOF analysis nor the Pearson correlation analysis shows a significant relation between
25 the ice core data sets and the instrumental rainfall data. In the EOF analysis the 4 ice core records
26 have high loadings only in 4 individual EOFs, respectively, and there is no relation with the
27 rainfall data. The highest Pearson correlation coefficients between ice core and rainfall data were
28 obtained for ER accumulation and North West India (NWI, $r=0.2$) and West Peninsula India (WPI,
29 $r=0.2$) rainfall, and for DSP and North Central India (NCI, $r=-0.25$). This explains only 4% and
30 6% of the variance in the core data. The highest correlation coefficient $r=-0.39$ between ice core
31 data is reported from DSP-accum and DSP- $\delta^{18}\text{O}$. This negative correlation points to amount effect,
32 typical for monsoon contribution, in contrast to the interpretation that DSP- $\delta^{18}\text{O}$ is influenced by
33 the temperature effect. The negative correlation between ER- $\delta^{18}\text{O}$ and precipitation amount along
34 the southern slope of the central Himalayas, as stated in the abstract, is not supported by the
35 correlation analysis with the rainfall data over India. There is just a weak anticorrelation with the
36 GPCC dataset.

37 To further verify precipitation seasonality along the Himalayas inferred from the climatological

38 observations from the four Himalayan weather stations, spatial distribution of non-monsoon
39 season (October to May) precipitation ratio to annual precipitation over the study area is
40 calculated using a high resolution reanalysis data (Fig. 4). It is clear that the non-monsoon season
41 precipitation ratio over the western high Himalayas (40-80%) is higher than that over the southern
42 and northern slopes of Himalayas (<20%), suggesting that local capture of the westerlies moisture
43 by mountain topography (western high Himalayas) is evident. Furthermore, the non-monsoon
44 precipitation ratio seems to gradually decrease from the western to central Himalayas due to
45 moisture wastage by sequential condensation of the westerlies moisture during its being
46 transported eastward. In the central Himalayas, however, the non-monsoon precipitation ratio is
47 highly changeable in the place that the Dasuopu and the ER ice cores are located. For instance, the
48 non-monsoon precipitation ratio at the Nyalam weather station (nearby Dasuopu core) can reach
49 53%, while the ratio at the Dingri weather station (nearby ER core) is less than 10%. The highly
50 variable non-monsoon precipitation ratio over the central Himalayas, in other words, the
51 remarkable discrepancy of the non-monsoon precipitation ratio between Dasuopu and ER, is likely
52 due to their local topographic features. The Dasuopu drilling site is located on the Mt.
53 Shishapangma ridge, which extends in a northwest-southeast direction, facing relatively low
54 terrains in the south and in the west (Fig. 1b). This provides a broad space for the western
55 disturbances invading and developing. Moreover, the northwest-southeast ridge of Mt.
56 Shishapangma is diagonal to the westerly flow, which is favorable for interacting with the western
57 disturbances, probably leading to significant wintertime precipitation at the Dasuopu drilling site.
58 On the other hand, the ER core was retrieved from the East Rongbuk Col on the northeast ridge of
59 Mt. Qomolangma (Everest). The very high west and southeast ridges of Mt. Qomolangma
60 (Everest) (Fig. 1b) may constrain the western disturbances in the southern slope of Mt.
61 Qomolangma (Everest) ridges, resulting in less wintertime precipitation at the ER drilling site.
62 Therefore, the ER drilling site is equivalently situated in the leeward slope (rain shadow region) of
63 the western disturbances, in contrast to the Dasuopu drilling site that is heavily influenced by the
64 western disturbances.

65 In the revision, we therefore suggest that different precipitation seasonality due to different local
66 topographical features between the DSP and the ER drilling sites may account for the different
67 interpretation of these two ice core stable isotopic records. In Figs. 5-9, we further analyze the
68 influence of the westerlies (ISM) on the DSP (ER) ice core records, which support our
69 conclusions.

70 In the revision, we find the ISM (westerlies) intensity varied substantially over time due to climate
71 changes over the past two centuries (Fig. 2). For instance, the relatively low ER accumulation rate
72 with small variation amplitude before the late 1930s is likely indicative of the ISM weakening; the
73 gradually decrease in Dasuopu accumulation rate under the ISM intensifying condition since the
74 late 1930s suggests the westerlies weakening during this period. Under the weak ISM condition,
75 wind scouring or sublimation of snow may be involved at the ER core site, although it is hard to
76 be quantified. Therefore, weak correlation between the ER ice core records and the instrumental
77 rainfall data in India before the late 1930s is probably due to wind scouring or sublimation of snow.
78 Otherwise, the westerlies (ISM) weakening (intensifying) since the late 1930s may weaken the
79 relationship between the DSP ice core records and the westerlies. The following two tables present
80 the correlation coefficients between the Himalayan ice-core records and the summer monsoon

81 rainfall of four Indian homogenous rainfall regions north of 21°N (NEI, NCI, NWI and NMI). We
 82 chose the four northern Indian rainfall regions since these monsoon-impacted regions are directly
 83 adjacent to the Himalayas. The correlation analysis of Table S1 and Table S2 supports our
 84 assumptions.

85
 86 The narrow band negative correlation region along the southern slope of Himalayas between the
 87 ER $\delta^{18}\text{O}$ and the summer precipitation (Fig. 9) doesn't overlap with the positive correlation region
 88 in the northwest India between the ER accumulation rate and the summer precipitation (Fig. 8).
 89 This suggests that the ER $\delta^{18}\text{O}$ is probably controlled by precipitation processes associated with
 90 deep convective activities over the southern slope of Himalayas due to its very steep topographic
 91 gradient, where the heavy isotopes in vapor are washed out strongly by intense precipitation
 92 processes.

93
 94

95 **Table S1.** Pearson correlation coefficients between the Himalayan ice cores records ($\delta^{18}\text{O}$ and
 96 accumulation rate) and the summer monsoon rainfall of four Indian homogenous rainfall regions
 97 north of 21°N (NEI, NCI, NWI and NMI) before the late 1930s (the year 1938). We choose the
 98 year 1938 as a boundary because the ER accumulation rate started to increase significantly since
 99 1938.

| | NEI | NCI | NWI | NMI | ER- accum | DSP- accum | ER- $\delta^{18}\text{O}$ | DSP- $\delta^{18}\text{O}$ |
|----------------------------|--------|---------------------|--------|--------|--------------|---------------|------------------------------|-------------------------------|
| ER-accum | 0.053 | 0.149 | 0.098 | 0.069 | 1 | 0.033 | -0.196 ^b | -0.003 |
| DSP-accum | -0.072 | -0.101 | -0.082 | -0.069 | | 1 | -0.112 | -0.314 ^a |
| ER- $\delta^{18}\text{O}$ | -0.163 | -0.029 | 0.039 | -0.037 | | | 1 | 0.094 |
| DSP- $\delta^{18}\text{O}$ | -0.031 | -0.198 ^c | -0.011 | -0.073 | | | | 1 |

100 Note: 2-tailed test of significance is used. a: 99% confidence level; b: 95% confidence level. ER: East Rongbuk; DSP:
 101 Dasuopu.

102

103 **Table S2.** Pearson correlation coefficients between the Himalayan ice cores records ($\delta^{18}\text{O}$ and
 104 accumulation rate) and the summer monsoon rainfall of four Indian homogenous rainfall regions
 105 north of 21°N (NEI, NCI, NWI and NMI) since 1938.

| | NEI | NCI | NWI | NMI | ER- accum | DSP- accum | ER- $\delta^{18}\text{O}$ | DSP- $\delta^{18}\text{O}$ |
|----------------------------|--------|---------------------|--------------------|---------------------|--------------|---------------|------------------------------|-------------------------------|
| ER-accum | -0.19 | -0.053 | 0.270 ^b | 0.197 | 1 | -0.212 | -0.251 ^b | -0.015 |
| DSP-accum | 0.163 | 0.352 ^a | 0.053 | 0.159 | | 1 | 0.212 | -0.233 ^c |
| ER- $\delta^{18}\text{O}$ | -0.021 | 0.122 | -0.046 | 0.121 | | | 1 | 0.165 |
| DSP- $\delta^{18}\text{O}$ | -0.040 | -0.397 ^a | -0.184 | -0.237 ^c | | | | 1 |

106 Note: 2-tailed test of significance is used. a: 99% confidence level; b: 95% confidence level; c: 90% confidence level. ER: East
 107 Rongbuk; DSP: Dasuopu.

108

109 The manuscript gives a long discussion about the spatial pattern of the Indian Summer Monsoon,
 110 which reads like a review paper. It is not clear what is new. This could be condensed.

111 We agree that some parts concerning to the spatial fluctuations of the Indian summer monsoon
112 (the north-south and west-east seesaws) and their influence on the Himalayan ice core isotopic
113 records are little relevant to the paper's goal, which is also pointed out by the other two reviewers.
114 Thus, we decide to delete this content in the revision.

115 On the other hand, details of the ice core records are missing. What is the elevation of the sites?
116 How was the accumulation corrected for thinning? Are the $\delta^{18}\text{O}$ -data annual data are how were
117 they obtained, how many data points per year? What is the dating uncertainty? Can the dating
118 uncertainty explain the low correlation with the instrumental data?

119 Details of the ice core records were included in the revision.

120 The elevation of the DSP core is 7200 m a.s.l. and 6518 m a.s.l. of the ER core.

121 Annual accumulation rate record of DSP core was constructed using a two-parameter steady state
122 flow model that takes into account the rapid thinning of annual layers near a glacier's flow divide
123 (Davis et al., 2005). And Kaspari et al (2008) developed a flow model to construct the ER core
124 annual accumulation rate record based on the annual-layer thickness data.

125 Annual $\delta^{18}\text{O}$ value is calculated by average of individual $\delta^{18}\text{O}$ values within a year.

126 The DSP core was annually dated back to 1440 AD at 144 meters, with an uncertainty of 3 years
127 (Thompson et al., 2000; Davis et al., 2005). Dating uncertainties of the ER core are estimated to
128 be ± 0 years at 1963 (20 samples per year) and ± 5 years at 1534 AD (4 samples per year) (Kaspari
129 et al., 2007).

130 Dating uncertainties of the Himalayas ice cores are probably not the main reason for the low
131 correlation with the instrumental data. The most possible reason may be the difference in
132 precipitation between the low Indian monsoon region and the high Himalayas.

133 This missing correlation with instrumental rain data suggests that they are not representative for
134 the conditions at the ice core sites, which might be very local due to the topography. Local effects
135 like wind erosion, melting, sublimation etc on the glacier are not considered at all. How does the
136 local topography look like, show maps. Does this favor wind erosion? Is here any information
137 about seasonality of precipitation at the sites?

138 Three-dimensional topographic maps of the DSP and ER glaciers are shown in Fig. 1b. As
139 indicated in our previous replies, we think that different precipitation seasonality due to different
140 local topographical features between the DSP and the ER drilling sites may be the main reason for
141 the different interpretation of these two ice core stable isotopic records. Local effects like wind
142 erosion and sublimation may be involved during the period before the late 1930s at the ER core
143 site as we mentioned before, but which are not the main reason for the different interpretations of
144 the two Himalayan ice core records. Ice core borehole temperature in the ER core from -8.9°C at
145 10 m to a minimum of -9.6°C at 20 m, then warmed slightly to -8.9°C at the bottom. The relatively
146 low temperature suggests that snow melting and snowmelt infiltration at the ER site may be not
147 important.

148 Information about precipitation seasonality at the two sites is absent due to the lacking of
149 meteorological observations at these high sites.

150

151 The trend in accumulation is extremely strong for both sites (more than 100% change). This seems
152 to be much larger trend than in the precipitation data, given e.g. in Yao et al., NCC 2012. Is this a
153 problem with thinning correction?

154 Both the DSP and ER accumulation rate records are constructed based on flow model. Thus this is
155 not a problem with thinning correction. Variation amplitude in precipitation given in Yao et al
156 (2012) is obtained based on precipitation data over a shorter period (1979-2010), which may be
157 small due to gentle climate change over the shorter period.

158 The interpretation that DSP receives significant contribution of precipitation associated with the
159 Westerlies is in contradiction with previous studies, which is not sufficiently discussed in the
160 manuscript. ER accumulation resembles most the accumulation reconstructions from Dunde,
161 Guliya, and Puruogangri ice cores, and the Tibetan Plateau precipitation, as given in Kaspari et al.,
162 J Glac, 2008. DSP shows a very different trend. It seems unlikely that a glacier so far North as
163 Dunde receives a significant Indian summer monsoon contribution, suggesting that the monsoon
164 contribution is higher at DSP. This is consistent with the sulphate record from DSP, which shows
165 the trend expected for Southern Asia (Duan et a., GRL 2007). At ER, the excess sulphate
166 concentration does not exhibit any trend or anthropogenic influence (Kaspari et al., JGR 2009). A
167 strong influence of the monsoon at DSP was also reported by Vuille et al., JGR 2005, who
168 detected a significant correlation between NCEP-NCAR JJAS monsoon index Mobs with annual
169 $\delta^{18}\text{O}$ values from DSP ice core between 1950 and 1996.

170 The discussion about our results comparing with previous studies has been added in the revision.

171 In Fig. 2, we can see clearly that the ER accumulation rate started to increase significantly since
172 1938, which corresponds well with remarkable increase in the ISM intensity. The average
173 accumulation rate of the ER core since 1938 is 0.65 m i.e. /year and the average value 1.00 m i.e.
174 /year of the DSP core. Modern meteorological observations from the Himalayan weather stations
175 and the NCEP/NCAR reanalysis data (Figs. 3 and 4) indicate that the non-monsoon precipitation
176 associated with the westerlies at the DSP site can reach 50% of its annual precipitation. This
177 means that about half precipitation (0.5 m i.e. /year) comes from the Indian summer monsoon at
178 the DSP site. On the other hand, about 90% of annual precipitation at the ER core site, that is, 0.59
179 m i.e. /year mainly derives from the Indian summer monsoon. Thus, the summer monsoon
180 precipitation amount at the two ice core sites is basically consistent. But the difference in
181 wintertime precipitation associated with the westerlies between the DSP (about 0.5 m i.e. /year)
182 and the ER (about 0.06 m i.e. /year) is remarkable, which would lead to pronounced differences
183 between the DSP and ER ice core records.

184 The debate on the influence domain of the summer monsoon is an open question. For instance,
185 Chen et al (2012) indicated that the Asian summer monsoon fringes (including the Indian
186 Monsoon and East Asian Monsoon) can reach the area north of the Tibetan Plateau during the
187 mid-Holocene (Figure S1 of their paper). The discussion about the monsoon domain is beyond the
188 scope of this paper.

189 The excess sulphate concentration in ER core does not exhibit any trend or anthropogenic
190 influence, which is likely because the SO_4^{2-} signal is dominated by dust (Kaspari et al., 2009).

191 Besides, there are many factors (for example, the dry/wet deposition) that can influence the
192 sulphate concentration in ice cores. Discussion about this is also beyond the scope of this paper.

193 We never deny the ISM contribution to precipitation at DSP. About half precipitation at DSP
194 originating from the ISM during the recent decades makes the result of Vuille et al (2005)
195 understandable. In this paper, we give some further interpretations for the difference between the
196 DSP and ER ice core records. Our conclusions, of course, are not final words, and more works
197 should be paid on this issue.

198

199 **References**

200 Cheng, H., et al. The climate cyclicity in semiarid-arid central Asia over the past 500,000 years.
201 *Geophys. Res. Lett.*, 39, L01705, doi:10.1029/2011GL050202, 2012.

202 Davis, M. E., Thompson, L. G., Yao, T., and Wang, N.: Forcing of the Asian monsoon on the
203 Tibetan Plateau: Evidence from high-resolution ice core and tropical coral records, *J.*
204 *Geophys. Res.*, 110, D04101, doi:10.1029/2004JD004933, 2005.

205 Kaspari, S., Hooke, R., Mayewski, P. A., Kang, S., Hou, S., and Qin, D.: Snow accumulation rate
206 on Mt. Everest: synchronicity with sites across the Tibetan Plateau on 50-100 year timescales.
207 *J. Glaciol.*, 54(185), 343-352, 2008.

208 Kaspari, S., Mayewski, P. A., Handley, M., Kang, S., Sneed, S., Hou, S., and Qin, D.: Recent
209 Increases in Atmospheric Concentrations of Bi, U, Cs, S and Ca from a 350-Year Mt. Everest
210 Ice Core Record, *J. Geophys. Res.*, 114, D04302, doi: 10.1029/2008JD011088, 2009

211 Kaspari, S., Mayewski, P. A., Kang, S., Sneed, S., Hou, S., Hooke, R., Kreutz, K., Introne, D.,
212 Handley, M., Maasch, K., Qin, D., and Ren, J.: Reduction in northward incursions of the
213 South Asian monsoon since 1400 AD inferred from a Mt. Everest ice core, *Geophys. Res. Lett.*,
214 34, L16701, doi:10.1029/2007GL030440, 2007.

215

216

217

218

219

220

221

222

223

224

225

226

227

228 **Tables and Figures in the revision**

229

230 **Table 1.** Pearson correlation coefficients between the Himalayan ice core records ($\delta^{18}\text{O}$ and
231 accumulation rate) and the summer monsoon rainfall of four Indian homogenous rainfall regions
232 north of 21°N (NEI, NCI, NWI and NMI) since 1813 AD.

| | NEI | NCI | NWI | NMI | ER-accum | DSP-accum | ER- $\delta^{18}\text{O}$ | DSP- $\delta^{18}\text{O}$ |
|----------------------------|--------------------|--------------------|-------------------|--------------------|--------------------|--------------------|---------------------------|----------------------------|
| NEI | 1 | | | | | | | |
| NCI | 0.19 ^b | 1 | | | | | | |
| NWI | -0.17 ^b | 0.46 ^a | 1 | | | | | |
| NMI | 0.01 | 0.54 ^a | 0.62 ^a | 1 | | | | |
| ER-accum | -0.10 | 0.02 | 0.20 ^b | 0.00 | 1 | | | |
| DSP-accumu | 0.01 | 0.01 | -0.09 | 0.02 | -0.31 ^a | 1 | | |
| ER- $\delta^{18}\text{O}$ | -0.12 | 0.03 | 0.02 | 0.01 | 0.01 | 0.10 | 1 | |
| DSP- $\delta^{18}\text{O}$ | -0.06 | -0.25 ^a | -0.02 | -0.15 ^c | 0.28 ^a | -0.39 ^a | 0.16 ^b | 1 |

233 Note: 2-tailed test of significance is used. a: 99% confidence level; b: 95% confidence level; c: 90% confidence level. ER: East Rongbuk;
234 DSP: Dasuopu.

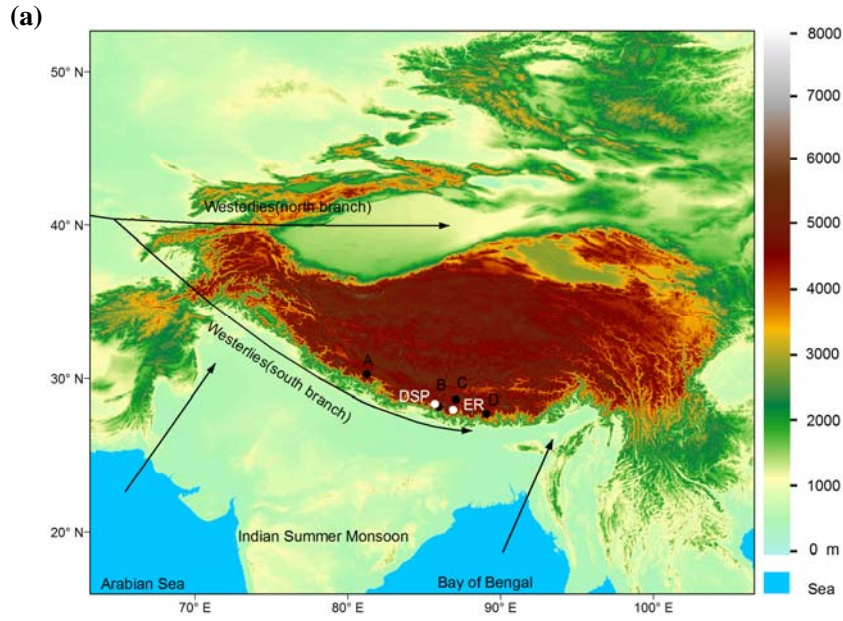
235

236

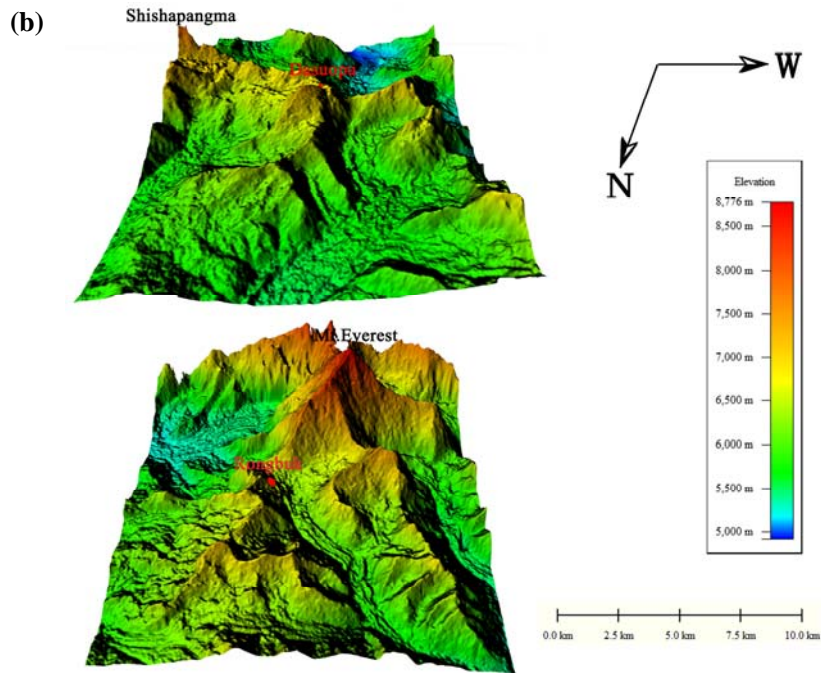
237

238

239

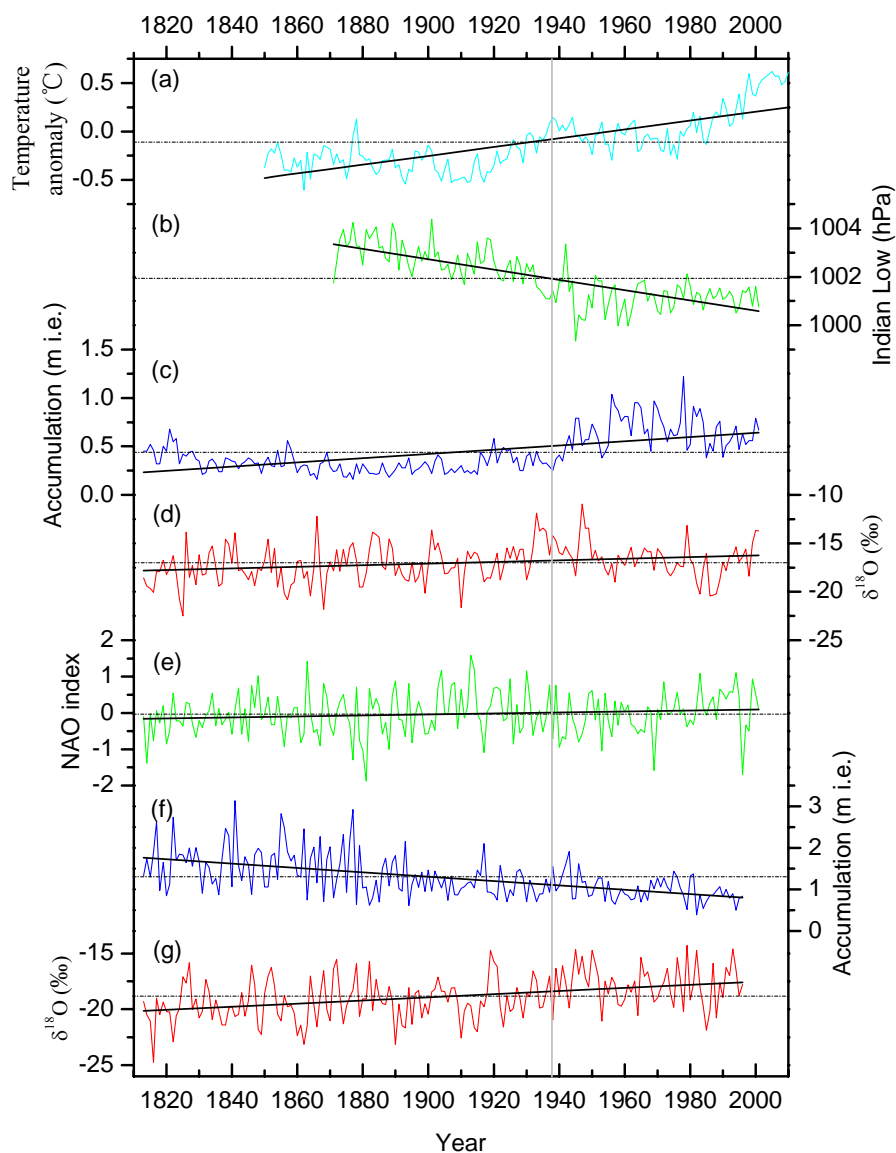


240



241

242 **Figure 1.** Atmospheric circulation systems over the study area (a), and three-dimensional
 243 topographic maps of the Dasuopu and East Rongbuk glaciers (b). Black solid circles indicate
 244 weather stations (A: Pulan; B: Nyalam; C: Dingri; D: Pali), and the white solid circles are the
 245 Dasuopu and ER ice core drilling sites. Digital elevation model (DEM) data is from ASTER
 246 (Advanced Spaceborne Thermal Emission and Reflection Radiometer) Global DEM with 30 m
 247 resolution.



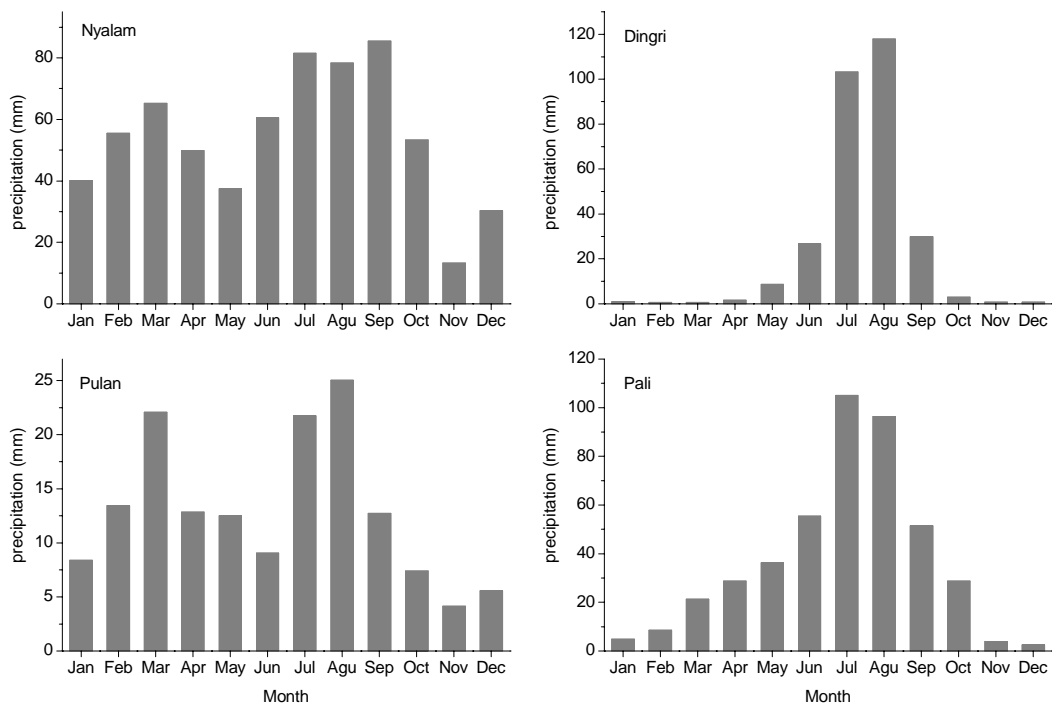
248

249 **Figure 2.** Variations of (a) Northern Hemisphere annual temperature anomaly (Jones et al., 2013),
 250 (b) the Indian Low intensity, (c) the ER annual accumulation rate, (d) the annual mean ER $\delta^{18}\text{O}$, (e)
 251 the non-monsoon season NAO index (Luterbacher et al., 2002), (f) the Dasuopu annual
 252 accumulation rate, and (g) the annual mean Dasuopu $\delta^{18}\text{O}$ since 1813 AD. The short dash dot lines
 253 are the averages of each series, and the bold lines are their linear trends. The vertical grey line
 254 indicates the boundary between the weak ISM period before the late 1930s (the year 1938) and the
 255 intensifying ISM period after the late 1930s. We choose the year 1938 as a boundary because the
 256 ER accumulation rate started to increase significantly since 1938.

257

258

259



260

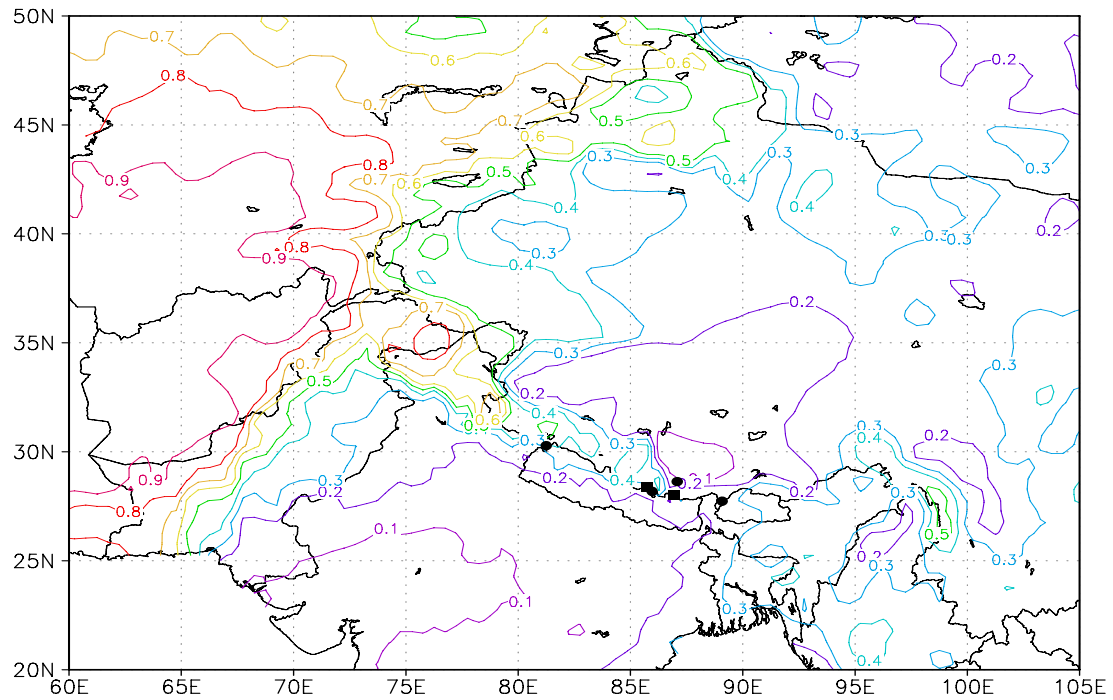
261 **Figure 3.** Monthly long term mean of precipitation at four weather stations along the Himalayas

262 (Nyalam, Pulan, Dingri and Pali). Seasonal distribution of precipitation is calculated based on the

263 meteorological data observed from January 1973 to January 2011.

264

265



266

267 **Figure 4.** Map showing the non-monsoon season precipitation ratios to annual precipitation

268 (October-May/annual) along the Himalayas. Reanalysis data are from the monthly long term mean

269 (1981-2010) precipitation data with a $0.5^\circ \times 0.5^\circ$ resolution from the Global Precipitation

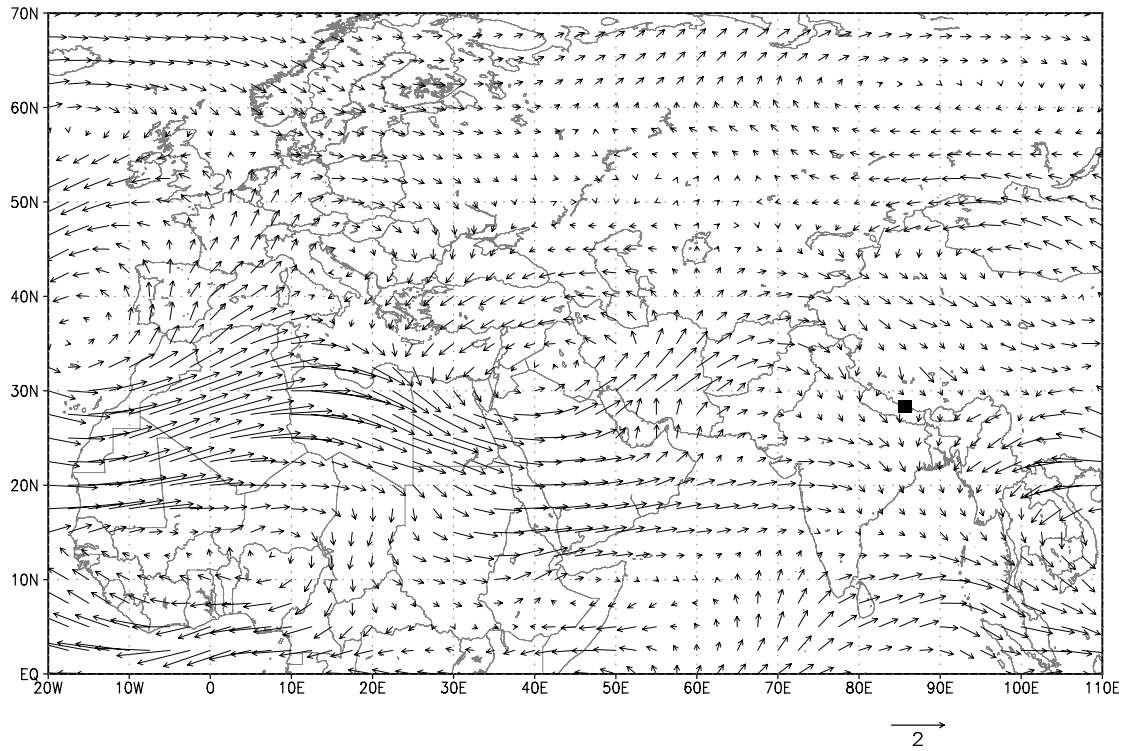
270 Climatology Centre (GPCC). Filled black circles are the four weather stations along the

271 Himalayas (from left to right: Pulan, Nyalam, Dingri and Pali). The non-monsoon precipitation

272 ratios at the Himalayan stations are generally consistent with those calculated from the GPCC data.

273 The filled rectangles are Dasuopu and East Rongbuk ice cores sites.

274



275

276 **Figure 5.** Composite analysis of moisture flux (multiplying by wind vector and specific humidity)

277 at 400 hPa level during the winter-spring season (February to April) between years with higher

278 and lower Dasuopu accumulation rate (higher-lower). The filled rectangle indicates the Dasuopu

279 core drilling site.

280

281

282

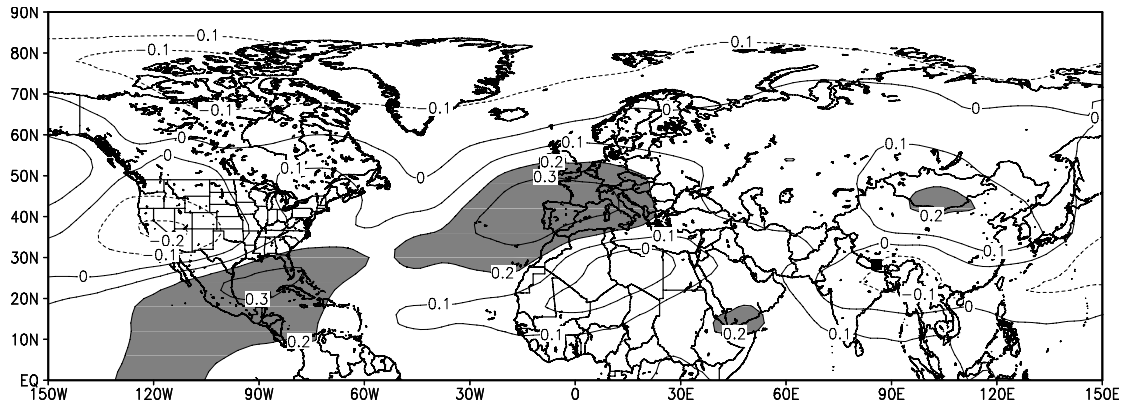
283

284

285

286

287



288

289 **Figure 6.** Correlation coefficients between the annual mean Dasuopu $\delta^{18}\text{O}$ and mean air
 290 temperature during the non-monsoon season (October to May) at 400 hPa level since 1871. The
 291 monthly air temperature data with $2.0^\circ \times 2.0^\circ$ resolution are from the twentieth century reanalysis
 292 (V2). Grey shadow indicates correlation significance at 95% confidence level. The filled rectangle
 293 indicates the Dasuopu core drilling site.

294

295

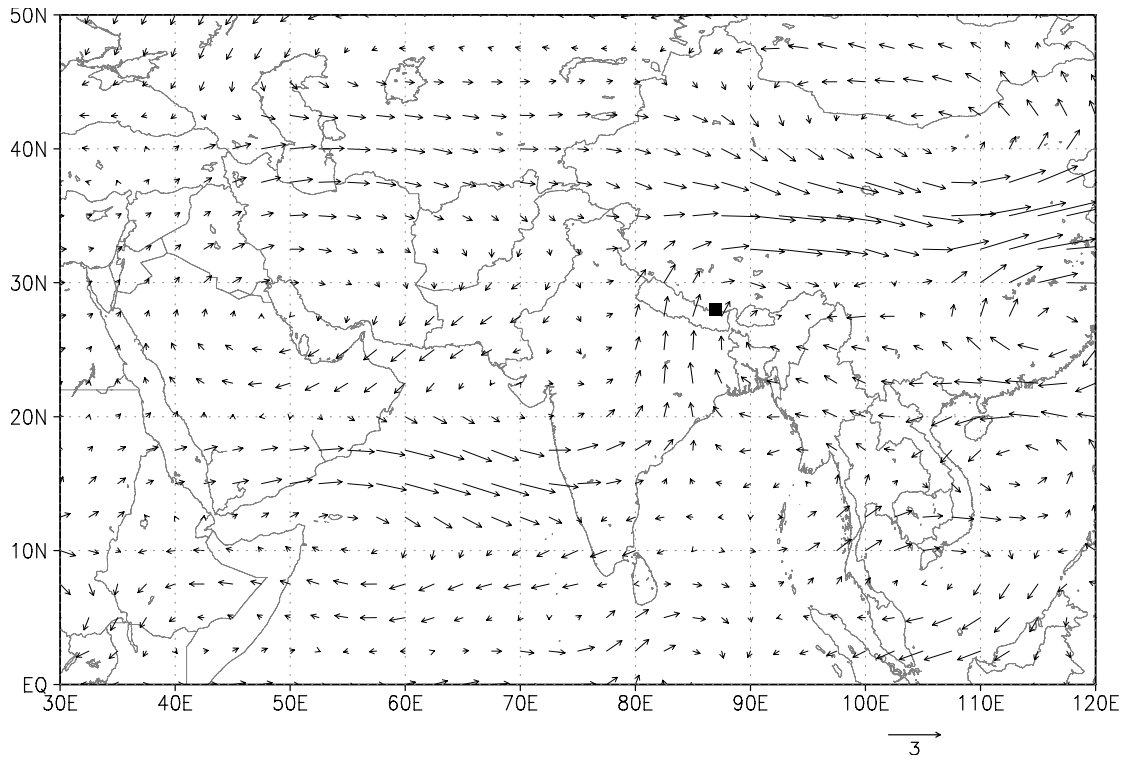
296

297

298

299

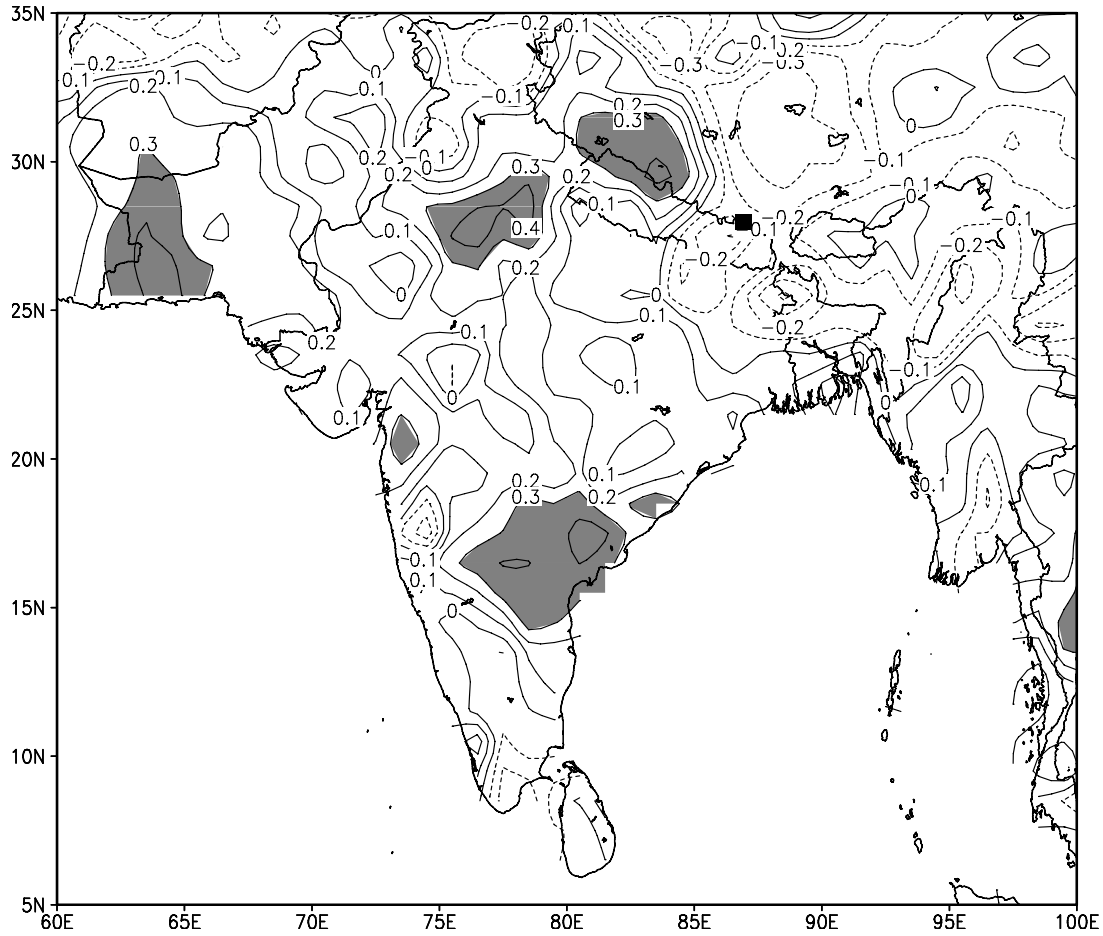
300



301

302 **Figure 7.** Composite analysis of summer mean (June to September) moisture flux (multiplying by
 303 wind vector and specific humidity) at 400 hPa level between years with higher and lower ER
 304 accumulation (higher minus lower). The filled rectangle indicates the ER core drilling site.

305



306

307 **Figure 8.** Correlation coefficients between the ER accumulation rate and summer (June to

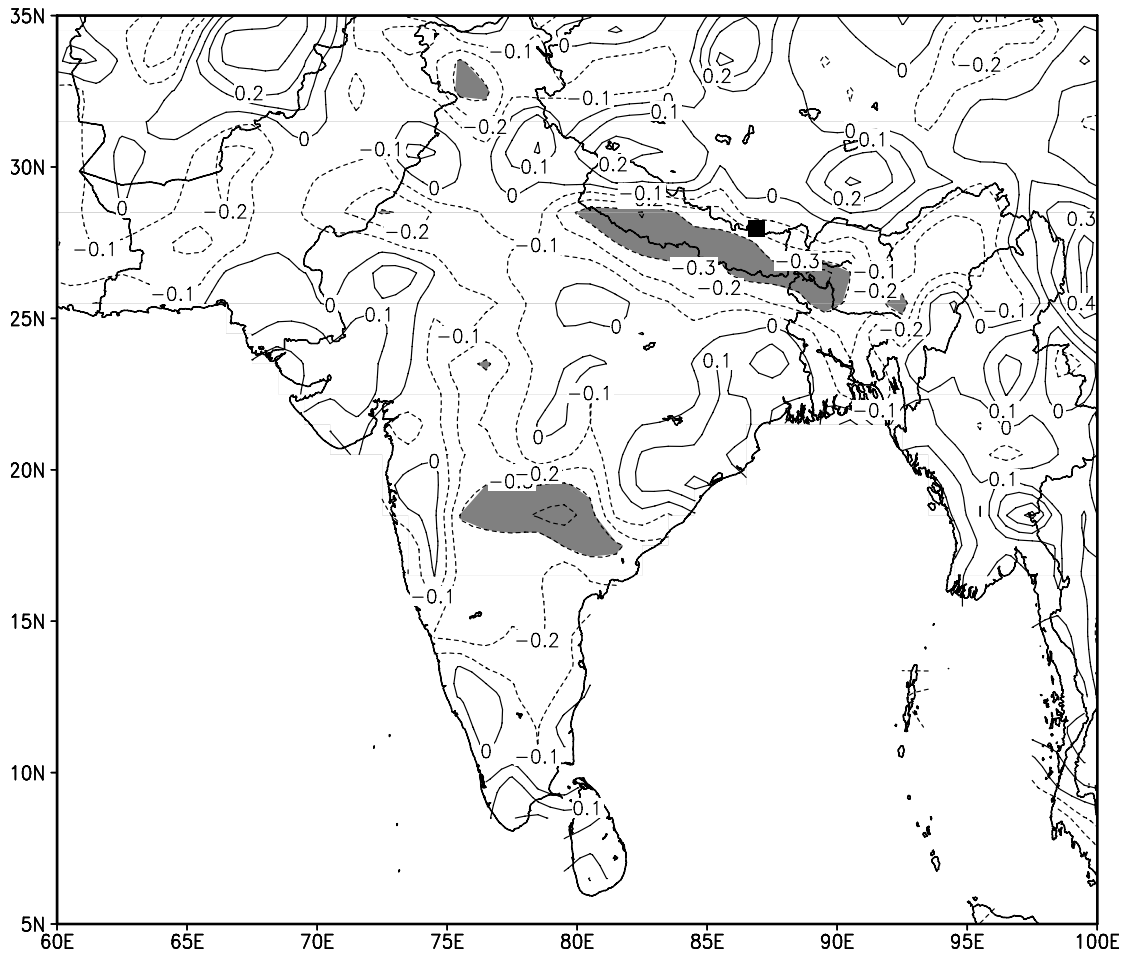
308 September) precipitation over the period 1951-2001. Grey shadow indicates correlation

309 significance at 95% confidence level. The filled rectangle indicates the ER core drilling site.

310 Summer precipitation data is from the Global Precipitation Climatology Centre (GPCC) monthly

311 precipitation dataset from 1951-present with $1.0^{\circ} \times 1.0^{\circ}$ resolution (available at <http://gpcc.dwd.de>).

312



313

314 **Fig. 9** Correlation coefficients between the ER $\delta^{18}\text{O}$ record and summer (June-September)
 315 precipitation over the period 1951-2001. Grey shadow indicates correlation significance at 95%
 316 confidence level. The filled rectangle indicates the ER core drilling site. Summer precipitation
 317 data is from the Global Precipitation Climatology Centre (GPCC) monthly precipitation dataset
 318 from 1951-present with $1.0^\circ \times 1.0^\circ$ resolution (available at <http://gpcc.dwd.de>).

319

320